New Laser Applications for Electric Propulsion

Mark W. Crofton†
The Aerospace Corporation
M5/754
2350 E. El Segundo Boulevard
El Segundo, California 90245-4691
310-336-1608
mark.w.crofton@aero.org

IEPC-01-305

Various applications of lasers to electric propulsion problems have previously been made, and laser techniques are potentially powerful means to address and resolve a range of current issues. Studies with sufficiently high resolution and sensitivity to reveal the fine details of velocity, density, and temperature distributions for trace species will be especially valuable. Continuous narrowband, coherent, tunable laser radiation in the ultraviolet region of the spectrum is often required to gain access to electronic transitions involving the ground state of the byproducts of thruster operation, as well as for propellant species themselves, but typically is generated with experimental difficulty. Means are presented to accomplish this task and enable the study of a large variety of previously unstudied species. The capabilities and applicabilities of two relevant laser systems are discussed in some detail. Previous applications of laser methods to electric thrusters are reviewed as well.

Nomenclature

A	radiative transition rate
g	statistical weight of quantum state
G	photomultiplier gain
h	Planck's constant
L	length of observation region
Q	quantum efficiency of detector
T	transmission of optics
V	excitation or scattering volume
λ_{ex}	wavelength needed for excitation process
λ_f	fluorescence wavelength
ν	transition frequency
Ω	optical solid angle

Introduction

Erosion, coupled with external deposition of highly divergent erosion products, is a common problem during the operation of electric thrusters. As a result of the erosion process, non-propellant species can be found at low levels in the plume. Electric thrusters tend to have this problem because of high energy deposition per unit mass flow and high voltage production of plasma that attains substantial density levels, coupled with local electric and magnetic fields that influence ionized particle migration in the plume. Detectable levels of Fe and Mo, from the discharge chamber and extraction grids, respectively, can be found in ion engine plumes. Detectable levels of the boron atom are expected to be present in Hall thruster plumes, produced by erosion of the boron nitride insulator. Sputtered anode materials may also be significant in the Hall thruster plume. Eroded species are the major source of spacecraft contamination for ion propulsion, and several other electric thruster types as well.

Metallic species are especially troublesome, because in some cases a film as thin as 10 Å may already produce unacceptable modification of surface properties. When ionized, particles can have a much higher probability of being found in

†Presented as Paper IEPC-01-305 at the 27th International Electric Propulsion Conference, Pasadena, CA, 15-19 October, 2001.

the backflow region and impinging on the body of the spacecraft, due to the local plume potential.

Lifetests conducted over periods of thousands of hours, or even the use of witness plates in hundred-hour exposures, are expensive and time consuming. Results in some plume locations may be spoiled by facility effects, since the tests are conducted in ground facilities. While quartz crystal microbalance detectors provide deposition rate information much more quickly, they also have issues in regard to facility effects and finer details - uncertainty exists concerning species identification and energy of impact, and there are difficulties in mapping the entire plume.

Laser spectroscopic techniques can avoid some of the difficulties of lifetest, witness plate, and QCM work. However, this approach can also become labor intensive and expensive, with issues of detection sensitivity, quantitative accuracy, and the installation of optical components near the thruster. Laser methods provide a high level of detail about certain aspects of the problem but may provide insufficient information in themselves concerning macroscopic behavior. In practice, the combination of two or even more diagnostics is advisable. Of the various possible diagnostics, the laser approach is the most complex and least developed – possibly due to the experimental difficulty combined with issues of facility and thruster availability.

Means to probe a wide variety of plume species using laser-induced fluorescence (LIF) are described in this report. These are based on the generation and use of tunable, narrowband laser radiation primarily in the ultraviolet region of the spectrum, 200-400 nanometers. Methods of generating and applying such radiation, and the two laser systems being put into use in the author's laboratory are discussed. The longest wavelength absorption involving the electronic ground state occurs in the uv, for most of the species of interest. By monitoring the transition, usually by laser-induced fluorescence, relative density and velocity maps can in principle be made for individual species. These include Mo, B, Fe, Ta, Ba, Ti, C, W, and even Xe^+ and Mo^+. In addition, flow fields and other properties can be determined.

Review of Previous Work

A substantial number of laser-based studies of electric thrusters have now been performed, with the arcjet, ion engine, Hall thruster, and resistojet having been the subject of at least one study each.

For the Hall thruster, excited electronic levels of Xe^+ have been probed by non-resonant LIF in the plume of SPT-100[1], SPT-140[2], and low power models.[3,4] Information about the near-field ion trajectories and velocity distributions was obtained.

For the ion engine, the ground state of molybdenum was probed by resonant LIF in the plume of a 30-cm, twin-grid ring cusp thruster[5] and of a 10-cm, triple-grid Kaufman-type engine.[6] Information was obtained about the density distribution and its dependence on operating point. In addition, the density distribution of Xe was measured in the plume of the 10-cm engine, using 2-photon laser absorption from the ground state and detection of fluorescence.[7]

For the resistojet, measurements of H_2 velocity distribution were made at precise locations inside the nozzle, using the coherent anti-Stokes Raman (CARS) technique.[8]

The largest body of laser-based work has been performed on arcjets, principally using the hydrogen atom as probe species. H atom velocity distribution in the lowest excited state was measured in high-power ammonia and low-power hydrogen arcjet plumes using a cw LIF technique.[9,10] A density measurement of the H atom ground state was performed in low-power ammonia and hydrogen arcjets via the absorption of pulsed xuv laser radiation.[11] A cw LIF study of H atoms was also conducted inside a hydrogen arcjet nozzle.[12] Two-photon studies of density and velocity distributions for H atom were performed in the plumes of hydrogen[13] and simulated hydrazine arcjets.[14] The H_2 molecule has been studied, with limited success, using a Raman technique. The density, velocity, and internal temperature distributions – rotational and vibrational - of the NH molecule (electronic ground state) have been studied via pulsed LIF in

simulated hydrazine[15] and ammonia[16] arcjet plumes. A few other arcjet studies have been performed as well on N atom and rare gas species. Metastable helium atoms were studied in absorption in the plume of a helium arcjet, using a near-infrared diode laser source.[17]

Each laser-based study of an electric thruster has produced highly specific information concerning plume properties. The overall result is best when such data are combined with other measurements made by various techniques, and incorporated into a high quality model of the system.

Apparatus

YAG-pumped dye laser system (pulsed)
A Spectra Physics Nd:YAG laser, model PRO-270 operating at 20 Hz, provides the pumping source for a Sirah Precision Scan-DA tunable pulsed dye laser. The dye laser utilizes dual 2400 line, 90 mm gratings for high resolution, and a second main amplifier for high pulse energy. Typical linewidth is below 0.04 cm^{-1}. For harmonic generation of the YAG fundamental to make 532 and 355 nm pulses, the output energy normally exceeds 600 and 350 mJ, respectively. Dye laser conversion efficiency is typically 13-22 % for the various dyes using 355 nm pumping, and 18-30% for 532 nm pumping.

The high energy output of the pulsed system enables efficient doubling or tripling of its frequency to generate tunable wavelengths as low as 195 nm. This is accomplished in KDP and BBO crystals tuned according to measured parameters used to create a scan lookup table. High pulse energy can be generated throughout the uv by this means. As an example, in excess of 10 mJ can be generated at 225 nm, the wavelength used previously for the determination of xenon density distribution in an ion engine plume by 2-photon LIF. However, in that case available pulse energy was only about 2 mJ. Since the signal depends on pulse energy squared until saturation is approached, a large enhancement of signal can be expected for that measurement. The narrow laser bandwidth can also be beneficial. A similar situation applies to the 2-photon LIF study of H atom with λ_{ex} of 205 nm. High available pulse energy also leads to the possibility of performing the first measurement of Xe^+ density, a difficult proposition due to the high energy of the lowest excited state (excited state Xe^+ density profiles are unlikely to mirror the total density profile),.

Ion-pumped ring laser system (cw)
A Coherent Sabre Ar^+ laser provides the pumping source for a Coherent 899-21 tunable ring laser. The Sabre has a dual Brewster-window configuration, with specified output power of 25 W all-lines visible or 7 W all-lines ultraviolet. The ring laser can use either a fluorescent dye or a titanium-doped sapphire (Ti:Sa) crystal as its gain medium. Using a birefringent filter as the sole tuning element the linewidth is typically below 10 GHz and the wavelength resettability is better than 0.1 nm (0.01 nm if using a wavemeter). With the intracavity etalons in place, active stabilization on, and with the frequency locked to an external reference cavity, the laser linewidth is ≤ 500 kHz and frequency drift is also low. The continuous scanning range goes up to approximately 1 cm^{-1}, at which point a manual reset is required in order to scan a new segment.

Operation using the Ti:Sa crystal is advantageous in terms of output power and stability, but disadvantageous in terms of system setup and beam alignment since the laser beam is invisible over most of the gain curve. Output power usually exceeds 1W. This gain medium is limited primarily to the 690 to 1050 nm range. If the Ti:Sa output is frequency doubled (operated narrowband so that linewidth is sub-MHz) wavelengths from 350 to 525 nm may be generated with conversion efficiency on the order of 10% with ~ 1W input, using an external cavity doubler system. A model MBD-200 doubler is used for this, also supplied by Coherent.

The ring laser wavelength is halved by the doubling process, extending its range down to 200 nm. In order to cover the full frequency range available, numerous optics sets are required. Each set is based on an LBO or BBO crystal. The critical region 360-420 nm can be accessed either by doubling the Ti:Sa output or through uv pumping of Exalite dyes, which lase directly over narrow segments within this region. Expected conversion efficiency is ≤ 1% for production of wavelengths in the 200-260 nm range, resulting in

≤ 1 mW after doubling. Frequency resolution of 1 MHz, a very small $\Delta\nu$ in comparison to the Doppler width, can be achieved even after doubling.

The doubler is essentially a Fabry-Perot enhancement cavity with an electronic control system to lock the cavity at maximum intracavity power. The Hansch-Couillaud locking technique is utilized, involving use of a polarization analyzer to monitor reflected light from the cavity. The enhancement in conversion efficiency associated with resonance vs. single pass is about three orders of magnitude.

Frequency calibration of the laser source can be difficult when the level of accuracy requires setting the laser source to overlap with a weak atomic or molecular probe transition. The accuracy needed may be ≤ 0.02 cm^{-1}, challenging the accuracy limit of most commercial wavemeters. Further difficulty may arise when the transition occurs at a shorter wavelength than 400 nm, the cutoff for many wavemeters. With a change of detector and optics some wavemeters will work well beyond 400 nm. The Burleigh cw models (WA-1000, WA-1500) fall into this category. However, it was found that these wavemeters read the ring laser wavelength when operated on Exalite 392E (using the visible optics and detector combination) with error bars of 0.1 to 200 cm^{-1}, the range of fluctuation depending on laser adjustment and noise in the dye jet.

Hollow cathode discharge lamps are readily available with a wide variety of cathode elements. In addition, a suitable gas fill can be selected to support frequency calibration requirements. To provide a frequency calibration source for a metal atom, a hollow cathode lamp would simply be utilized with that metal constituting the cathode material. Detection of an atomic line depends on the optogalvanic effect. A change in the discharge parameters may be more difficult to detect with a cw laser source, particularly if at low power level. In addition, the discharge sensitivity to the various atomic transitions varies substantially, and not all are detectable.

When neither a wavemeter or hollow cathode lamp are sufficient for the task at hand, a variety of condensed species can be generated in the gas phase in abundance by pulsed laser vaporization. The resultant atoms or molecules can then be probed via laser-induced fluorescence or an alternate technique. The experimental setup employed in a frequency calibration for molybdenum spectroscopy is illustrated in Fig. 1. A 20 Hz Q-switched Nd:YAG laser was frequency tripled, and about 30 mJ of the 355 nm pulse was split off and focused on a molybdenum target mounted in an evacuated cell. Tunable laser light at about 390 nm was passed through the cell above the target. Optics were placed as shown in Fig. 1 to collect any resonant fluorescence emitted while the laser frequency was swept. The laser frequency was approximately determined by a Burleigh WA-4500 cw/pulsed wavemeter whose specified accuracy is ± 0.02 cm^{-1} over the 400-1100 nm range. Due to the optical dispersion below 400 nm the wavemeter reading was incorrect by more than 10 cm^{-1}. The fluorescence signal was collected and monitored during a ~10 μs window commencing ≥ 1 μs following the laser pulse to reduce the detected light scatter. Due to the broad velocity distribution of the molybdenum atoms the excitation spectral profile was broadened, and dependent on the observation window.

Pulsed laser vaporization coupled with laser-induced fluorescence has previously been applied to barium.[18] The density was high enough to permit use of planar LIF to image the expanding plume. It does not appear that similar studies have been performed on most of the other species discussed here. The velocity and particle mass distributions resulting from laser vaporization or ion sputtering from material surfaces used in thrusters are of interest in their own right.

Techniques and Applications

A partial list of laser-based techniques includes CARS, Raman, Rayleigh Scattering, MPI (Multi-Photon-Ionization), Absorption Spectroscopy (XUV, cavity ring-down, and more conventional approaches), degenerate four-wave mixing, and laser-induced fluorescence. Only a few of these are appropriate for electric thruster measurements. Additional discussion has appeared elsewhere [19].

For species present in an electric thruster plume at very low density, 10^5 to 10^8 cm^{-3}, LIF is virtually the only convenient means of detection. Other techniques have sensitivity problems because of the low density and noisy environment. For example, the MPI detection limit can be as low as 1 cm^{-3} under ideal circumstances, but the plasma background and inability to efficiently extract ions formed by the laser pulse (at least not without disturbing thruster operation) greatly reduce the sensitivity of the method. In addition to its sensitivity advantage, LIF also has very good spatial

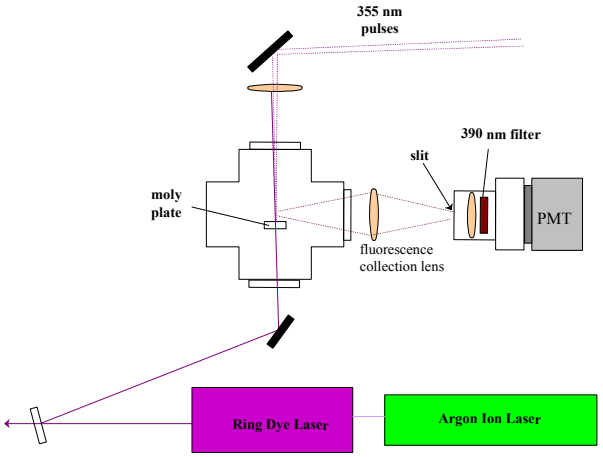

Figure 1. Schematic diagram of experimental setup for frequency calibration on a molybdenum transition.

resolution. A comparison of continuous (cw) and pulsed LIF methods indicates that the cw approach is usually preferable on the basis of sensitivity and spectral resolution considerations. The difference in duty factor accounts for the fact that cw sensitivity is usually higher. When sensitivity is not an issue, the pulsed system may be preferred due to generally better spectral coverage with less effort required.

For a three level system involving absorption from level 1 to 2, and fluorescence from 2 to 3, if the upper level 2 is saturated by a laser pulse the fluorescence signal will be independent of the laser intensity. The peak fluorescence signal power is then related to the concentration of the particle species, in the absence of collisional quenching, by[20]

$$P_{23}^{\max} = \frac{h\nu_{23}}{4\pi} A_{23} NV \frac{g_2}{g_1 + g_2} \Omega GTQ \qquad (1)$$

After the detection system is calibrated from the intensity of collected Rayleigh scattering, the absolute density of the fluorescing species can be determined. This approach cannot be used with cw LIF, however.

YAG-pumped dye laser system (pulsed)
The pulsed approach has already been utilized to study many of the plume species of interest that it is suitable for: H atom, NH molecule, Xe atom, and H_2 molecule (see discussion of previous work). A pulsed system is not as amenable as a cw laser to the study of trace species.

N_2 Neither H_2 or N_2 has been studied in operating electric thruster plumes. These molecules are particularly important for improving understanding of arcjet operation. Means to characterize these species are of interest in science and engineering in general, but this is an especially difficult proposition for N_2. Although nitrogen has been successfully studied in some environments by 2-photon LIF of the a $^1\Pi_g \leftarrow X\ ^1\Sigma_g^+$ band, the 140 μs lifetime of the upper state results in prominent fluorescence quenching effects in arcjet plumes.[21] The solution seems to be a more elaborate LIF setup involving the generation of tunable xuv pulses to excite a short-lived upper state by one-photon absorption.

H_2 H_2 can be studied via 2-photon LIF using the E $^1\Sigma_g^+ \leftarrow$ X $^1\Sigma_g^+$ (0-0) band. Only the 0-0 band mirrors the ground state rotational population.[22] Fortunately, this band is centered at λ_{ex} ~ 201 nm, within the convenient range where frequency conversion can be accomplished in a BBO crystal. The upper state fluoresces to the B $^1\Sigma_u^+$ state in the near infrared. Except for minor changes in the excitation and fluorescence wavelengths, the experimental setup for H_2 2-photon LIF would be similar to that previously used for H atom (see Fig. 2).

Xe^+ Excitation from the ground state of singly ionized Xe^+ for LIF has not been performed in any

system, electric thruster or otherwise. Due to the high excited state energies and the incompatibilities for 2-photon absorption in accessible wavelength regions, the best candidates for population of a fluorescing excited state appear to involve 3-photon excitation. One scheme involves the transition $5s^25p^4(^1S)6s\ ^2S_{1/2} \leftarrow 5s^25p^5\ ^2P_{3/2}{}^0$ with λ_{ex} = 232.11 nm (see Fig. 3). The upper state is given in LS notation, but JK coupling could also be used since the upper state composition is highly mixed. Because xenon is a large atom the common selection rules involving, for example, no change in spin multiplicity, are not rigorous. Due to this fact and lack of work on this species, there is uncertainty concerning what is the optimal approach for a practical Xe^+ LIF scheme. For the transition given above, a good candidate for fluorescence monitoring is the 572.86 nm line, which involves a transition to $5s^25p^4(^3P)6p\ ^4P_{3/2}{}^0$. Because the excitation involves 3-photon absorption, high density coupled with high pulse energy and tight focusing is mandatory. The technique can be developed in a dense plasma environment, then transitioned if feasible to the study of an ion thruster. The discharge channel of a high power Hall thruster contains Xe^+ ions in considerable abundance, therefore this is a promising location for first application. If successful, detailed information concerning density and velocity mappings can be generated. Obviously, however, a much easier way to obtain velocity information is through cw LIF involving metastable Xe^+, as previously performed.[1-4]

Ion-pumped ring laser system (cw)

H atoms and molybdenum atoms are the species previously studied in thruster plumes using a ring laser, but there are many other candidate species.

Mo In both of the previous studies, resonant LIF was performed on the z $^7P_2{}^o \leftarrow$ a $^7S_3$ transition at 390.41 nm. The effects of accelerator grid voltage and propellant utilization were examined in particular. The laser resolution was on the order of 1 cm^{-1}, which lowers sensitivity in comparison to the high resolution case and did not allow the study of spectral profiles. As a result, velocity distribution and kinetic temperature were not obtained. Other LIF schemes could be used on Mo, for example a non-resonant approach with λ_{ex} = 319.49 nm (upper state y $^7P_2$) and fluorescence to the a $^5S_2$ state with λ_f = 487.05 nm.

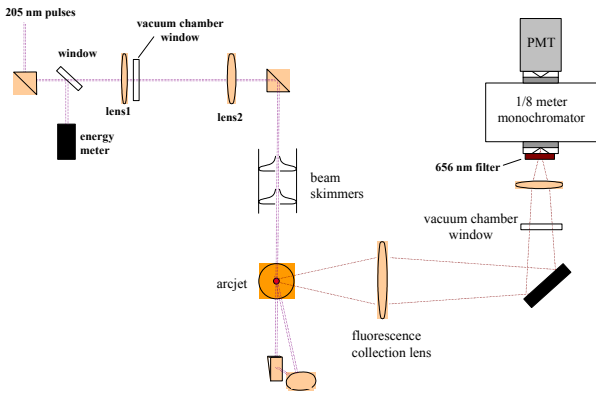

Figure 2. Schematic diagram of optical setup for 2-photon LIF study of H atom.

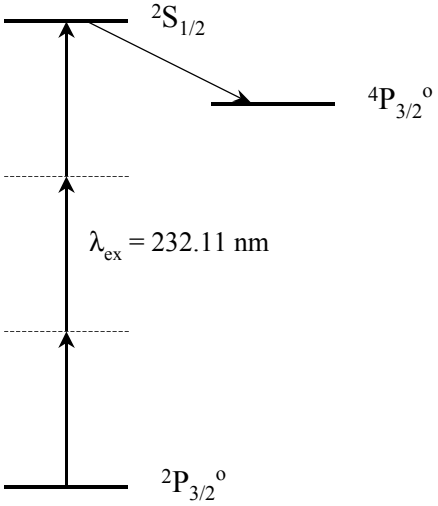

Figure 3. Schematic diagram indicating a proposed 3-photon LIF approach for Xe^+ detection.

Fundamental information concerning the ion and neutral relative abundance produced as a function of Xe^+ impingement energy on Mo, and the energy distributions of the sputtered species, is not available. This fact points to the need for a study of energy distribution and ionization fraction resulting from Mo sputtering in an idealized system, in addition to a high resolution ion engine plume study.

Ti Titanium has generated considerable interest as a grid material. Like Mo, Ti has transitions in the near ultraviolet that originate from the ground electronic state. Several candidate transitions for resonant LIF from the $^3F_2$ ground state are at λ_{ex} = 501.6, 395.0, and 390.0 nm (lifetimes of approximately 165, 16, and 15 ns, respectively).[23] There are others at shorter excitation wavelengths. The excited state y $^3F_3^o$ has a radiative lifetime of 17 ns and fluoresces non-resonantly at 735 nm, with an accessible transition from the ground state at 396.4 nm.[24] A number of transitions may therefore be suitable for laser-induced fluorescence monitoring in a gridded ion engine plume. Recently, LIF imaging of Ti and Ti^+ has been performed by absorption and LIF, respectively, at nearly identical wavelengths (~335 nm) and in the same plume of laser-vaporized material, to generate contour density maps.[25]

Ta Tantalum is frequently used in components where low sputter yield is required. One of these components is the hollow cathode, a device used in Hall-effect thrusters and gridded ion engines. These hollow cathodes are prone to single-point failures of the thruster system, and their operation is still poorly understood. Tantalum has never been monitored in a hollow cathode or electric thruster plume (there has been an LIF study of excited-state neutral Xe in a hollow cathode plume, however, see Ref. [26]). With a suitable laser spectroscopic technique, near-field monitoring could be very valuable in the scientific study of hollow cathodes.

Table 1. Selected tantalum transitions involving the ground electronic state.

Upper Level	λ_{ex} (nm)	λ_f (nm)
y $^4G^o_{5/2}$?	271.55	
z $^4P^o_{5/2}$?	340.79	543.68
y $^4D^o_{5/2}$	355.44	
z $^4P^o_{1/2}$?	372.22	
y $^4D^o_{1/2}$	391.96	R
z $^4D^o_{5/2}$	472.42	581.27, R
z $^4D^o_{1/2}$	540.40	R

There are several transitions in the uv and visible region from the a $^4F_{3/2}$ ground state of tantalum (see Table 1 and Ref. [27]), which may be suitable for monitoring this species.

Ba Barium is a critical species for the proper operation of most hollow cathodes used in ion engines. Like Ta, there has not been any laser-based study of plume barium in an electric thruster or component device. A brief mention of the detection of barium in a hollow cathode plume has appeared in the literature, but this was done in the far-field using a mass spectroscopic method.[28] Several approaches have been used successfully to monitor Ba in other systems. One approach is to observe resonance fluorescence at 553.5 nm, a transition with very high oscillator strength.[29] Observation with $\lambda_{ex} = \lambda_f$ = 350.1 nm can also be performed. A third approach utilizes λ_{ex} = 307.2 nm and λ_f = 472.8 nm.[18] Finally, an approach which may produce the highest signal to noise ratio involves excitation at 350.1 nm and observation of fluorescence at 582.6 nm.[30] Table 2 summarizes these approaches.

Table 2. Various laser-induced fluorescence schemes involving the $6s^2\ ^1S_0$ barium ground electronic state.

Upper Level	λ_{ex} (nm)	λ_f (nm)
6s 6p $^1P_1$	553.5	553.5
5d 6p $^1P_1$	350.1	350.1/582.6
6s 7p $^1P_1$	307.2	472.8
5d 6p $^1P_1$	350.1	582.6

B The boron atom is expected to be a prominent constituent in Hall thruster plumes, stemming from the ion sputtering of its boron nitride insulator material. BN molecules will also be produced in this process. Neither species has been detected in a Hall thruster plume by any direct means, although the monitoring of deposition products which include boron has been performed through the collection of deposition materials on witness plates, with subsequent removal and study by standard elemental analysis methods. Throughout most of the Hall thruster plume erosion dominates deposition, so that boron is removed as fast as it deposits. This fact increases the utility of direct boron detection within the plume as a diagnostic of thruster operation. The longest wavelength for an allowed electronic

transition originating from the $2p\ ^2P^o$ electronic ground state is at 249.85 nm, with upper state $2s^2\ 3s\ ^2S_{1/2}$.[31] This transition is a doublet, so it has a close neighbor. The excited state lifetime is just 4 ns due to the large oscillator strength of the transition.[32] The fluorescence occurs at the excitation wavelength.

Additional transitions occur near 209 nm and below.[31] While it is advantageous to use a higher frequency transition that produces fluorescence at a second, lower frequency, use of a cw laser at such short wavelengths is more difficult. The short wavelengths are more accessible using a pulsed laser system, but the boron density is probably too low to make this a feasible approach. Transitions exist at approximately λ_{ex} = 182 nm that conveniently fluoresce in the visible, but production of the excitation pulse requires the addition of a Raman shifter.[32]

Production of cw radiation near 250 nm is accomplished using uv pumping of a suitable dye such as coumarin 102 to generate wavelengths near 500 nm, and doubling this output with the MBD-200 external cavity doubler. Since the coumarin 102 single frequency output is ≤ 150 mW, the doubling efficiency is ≤ 1% and obtainable power at 250 nm is on the order of 1 mW or below.

BN The BN molecule will also be produced during the sputtering of condensed boron nitride. While the boron atom may be easier to detect, the study of BN can provide additional information. For example, rotational, vibrational, and translational energy distributions can reveal further information about local temperature.

It is the $A^3\Pi_i$-$X^3\Pi_i$ band of BN that is most suitable for study in the Hall thruster plume. Most of the 0-0 band falls within the region of 360 to 364 nm, with a very high density of transitions.[33]

W Tungsten is found more sparingly in ion thrusters, although it must be mentioned that the use of a tungsten filament to neutralize the ion beam is not uncommon and would result in a considerable abundance of this material in the plume. Tungsten has been the material of choice for the cathode of arcjets and magnetoplasmadynamic (MPD) thrusters, and also finds common use in the nozzle orifice of hollow cathodes. It is therefore an important plume constituent to be monitored.

Tungsten and its singly ionized form have previously been studied by pulsed LIF in vacuum arc plasmas.[34,35] Relative transition probabilities are known in most cases.[36] One potential scheme for cw LIF involves excitation to the z $^7D_1^0$ (21454 cm^{-1} or 465.987 nm) with detection of fluorescence at 505 or 551 nm. The upper state lifetime is approximately 275 ns, and the oscillator strength is moderate for both excitation and fluorescence.[37] A promising alternative scheme could utilize 255.135 nm excitation and non-resonant fluorescence detection, however this excitation wavelength is considerably more difficult to generate.

Fe Iron is present in most thrusters, in discharge chambers, magnetic pole pieces, and other components. Iron can undergo laser-induced fluorescence using a 248.327 nm wavelength, very close to λ_{ex} for boron, to excite atoms from the a $^5D_4$ ground state. Although this approach may not have been tried previously for LIF, it is a commonly used transition for atomic absorption. A number of other LIF schemes have been proposed or utilized, most involving pulsed LIF at λ_{ex} ~ 300 nm.[38,39] The first direct measurement of the velocity distribution of excited atoms sputtered from a metal target was done on the a $^5F_5$ metastable state of Fe at 0.86 eV.[40] The velocity distribution was found to be much more broad and peaked at higher energy for the excited atoms as compared to ground-state species.

C Carbon atoms are often abundant in the plume during ground testing because the beam stop and/or test chamber wall is made from or lined with carbon- containing materials. Carbon has been detected via 2-photon excitation, with one process using 246 nm pulsed radiation for excitation followed by fluorescence detection at 476.7 nm.[41] This approach may not have sufficient sensitivity for carbon at the typical plume density of ion thrusters.

Trace Ions Trace species in electric thruster plumes are usually produced by ion sputtering from component surfaces. While neutral species normally dominate, some fraction of the population will be ionized. The neutrals have some probability to become ionized in the plume, but the majority of ions are expected to arise from the sputtering process itself unless they originate in the discharge chamber. An ion has a much higher probability of being found at the largest angles with respect to the thrust axis, given the same initial velocity and density distributions at the source. This is due to the presence of electric fields that act to establish trajectories in radial and upstream directions, enhancing ion flux levels in the sideflow and backflow regions and ultimately accounting for the majority of contaminant flux backflowing to the spacecraft. The direct monitoring of trace ions is therefore of considerable interest, in addition to the neutrals.

Suitable excitation wavelengths for ground state ions are even further toward the blue end of the spectrum than for ground state neutrals, due to the higher electron binding energy. However, some ions are nevertheless amenable to study by cw LIF. While the velocity distributions of excited state species in plume electric fields are probably a reasonable approximation to the ground state distributions, because of the reduced density of ions those transitions involving the ground state are again preferred on the basis of their detectability, other factors being equal. Selected wavelengths for the excitation and detection of trace ions and the other species discussed are listed together in Table 3.

Mo^+ is considered to be the most important ion in the plume of a gridded ion engine that uses molybdenum ion optics. Fe^+ may also be of considerable importance, however, and Ti^+ would obviously be the target species if the grids were constructed from titanium. For Hall thrusters, B^+, C^+, Fe^+, and La^+ are possible ions of interest.

Only Fe^+ has previously been detected in an electric thruster plume, and this by a time-of-flight mass spectroscopic method in the far-field. Many of the ions discussed above may possibly be detectable by LIF despite the low plume densities that exist. The degree-of-difficulty is high, however. Mo^+ can be used as an example. The longest wavelength for a transition originating from the ground state is at 202.030 nm, a difficult region for generating cw tunable laser output. The most feasible approach is expected to be Ar^+ uv pumping of the appropriate Exalite dye combined with frequency doubling in a BBO external cavity doubler. The efficiency of this process is very low, such that substantially less than 1 mW of tunable output can be expected at 202 nm.

The backflow region does have certain advantages, however. In the first place, the low plasma density and absence of high energy ions allows placement of fluorescence collection optics

Table 3. Selected wavelengths for the laser-induced fluorescence study of thruster species.

Species	Measurement Type	Excitation Wavelength, λ_{ex}	Detection Wavelength, λ_f
Mo	Resonant	390.41	390.41
Mo^+	Resonant	203.91/ 202.10	203.91/202.10
Ta	Res & non-res	391.96/540.40/472.42	R/581.27/R
Ti	Res & non-res	396.4/390.0	735/390.0
W	Non-resonant	255.135/465.987/384.86	Various
Fe	Resonant	248.327	248.327
Ba	Res & non-res	553.5/350.1/307.2	553.5/582.6/472.8
Xe	2-photon	225.51	484.47
Xe^+	3-photon	232.11	572.86
NH	Near-resonant	330-342	330-342
H_2	2-photon	201	Near IR
H	2-photon	205.14	656
BN	Near-resonant	360-364	360-364
B	Resonant	249.85/249.75	249.85/249.75

very close to the interaction region. In addition there is low emission background due to the plasma. With painstaking care given to the reduction of scattered light, resonant fluorescence may be detectable at a density of ~ 10^5 cm^{-3}. Since the Mo^+ density cannot be orders of magnitude above this, signal to noise ratio will be low. Non-laser methods may be more appropriate for the study of backflowing plume ions, although other approaches will have their own difficulties.

Concluding Remarks

There is much potential for the use of laser-based techniques, particularly laser-induced fluorescence, to address critical issues of spacecraft contamination, thruster lifetime, and physics of thruster operation. The application of the approaches described is difficult, however, due to labor-intensive experimental setups and low species densities within a non-ideal environment.

Acknowledgments

The preparation of this manuscript was supported by The Aerospace Corporation through its IRAD Program under contract no. F04701-00-C-0009. The author wishes to thank Brendan Brelsford for technical support in developing LabView control programs for the ring laser system.

References

1. Manzella, D.H., "Stationary Plasma Thruster Ion Velocity Distribution," AIAA Paper 94-3141, June 1994.
2. Beiting, E.J., and Pollard, J.E., "Measurements of Xenon Ion Velocities of the SPT-140 using Laser Induced Fluorescence," 3rd International Conf. on Spacecraft Propulsion Proceedings, Oct 2000, pp. 897-900.
3. Cedolin, R.J., Hargus, W.A Jr., Storm, P.V., Hanson, R.K., and Capelli, M.A., "Laser-Induced Fluorescence Study of a Xenon Hall Thruster," *Applied Physics B*, Vol. 65, 1997, pp. 459-469.
4. Sadeghi, N., Dorval, N., Bonnet, J., Pigache, D., Kadlec-Philippe, C., and Bouchoule, A., "Velocity Measurements of Xe+ in Stationary Plasma Thruster using LIF," AIAA Paper 99-2429, June 1999.
5. Gaeta, C.J., et al, "Erosion Rate Diagnostics in Ion Thrusters using Laser-Induced Fluorescence," *J. Propulsion and Power*, Vol. 9, No. 3, 1993, pp. 369-376.
6. Crofton, M.W., "Laser Spectroscopic Study of the T5 (UK-10) Ion Thruster," AIAA Paper 95-2921, June 1995.
7. Crofton, M.W., "Measurement of Neutral Xenon Density Profile in an Ion Thruster Plume," AIAA Paper 96-2290, June 1996.
8. Beiting, E.J., "Coherent Anti-Stokes Raman Scattering Velocity and Translational Temperature Measurements in Resistojets," *Applied Optics*, Vol. 36, No. 15, 1997, pp. 3565-3576.
9. Erwin, D.A., Pham-Van-Diep, G.C., and Deininger, W.D., "Laser-Induced-Fluorescence Measurements of Flow Velocity in High-Power Arcjet Thruster Plumes," *AIAA J.*, Vol. 29, 1991, pp. 1298-1303.
10. Liebeskind, J.G., Hanson, R.K., and Cappelli, M.A., "Laser-Induced Fluorescence Diagnostic for Temperature and Velocity Measurements in a Hydrogen Arcjet Plume," *Applied Optics*, Vol. 32, No. 30, 1993, pp. 6117-6127.
11. Pollard, J.E., "Arcjet Diagnostics by XUV Absorption Spectroscopy," AIAA Paper 92-2966, July 1992.
12. Storm, P.V., and Cappelli, M.A., "Fluorescence Velocity Measurements in the Interior of a Hydrogen Arcjet Nozzle," *AIAA J.*, Vol. 34, No. 4, 1966, pp. 853-855.
13. Wysong, I.J., and Pobst, J.A., "Quantitative Two-Photon Laser-Induced Fluorescence of Hydrogen Atoms in a 1 kW Arcjet Thruster," *Applied Physics B*, Vol. 67, No. 2, 1998, pp. 193-205.
14. Crofton, M.W., Moore, T.A., Boyd, I.D., Masuda, I., and Gotoh, Y., "Near-Field Measurement and Modeling Results for Flight-Type Arcjet: Hydrogen Atom," *J. Spacecraft and Rockets*, Vol. 38, No. 3, 2001, pp. 417-425.
15. Crofton, M.W., Moore, T.A., Boyd, I.D., Masuda, I., and Gotoh, Y., "Near-Field Measurement and Modeling Results for Flight-Type Arcjet: NH Molecule," *J. Spacecraft and Rockets*, Vol. 38, No. 1, 2001, pp. 79-86.
16. Crofton, M.W., Welle, R.P., Janson, S.W., and Cohen, R.B., "Temperature, Velocity, and Density Studies in the 1 kW Ammonia Arcjet Plume by LIF," AIAA Paper 92-3241, July 1992.
17. Welle, R.P., "Energy Distribution in the Plume of a Helium Arcjet," AIAA Paper 99-0453, Jan. 1999.
18. Capelli, M.A., Paul, P.H., and Hanson, R.K., "Laser-Induced Fluorescence Imaging of Laser-

Ablated Barium," *Applied Physics Letters*, Vol. 56, No. 18, 1990, pp. 1715-1717.

19. Crofton, M.W., "Advanced Diagnostic Techniques for Electric Propulsion," AIAA Paper 93-1794, June 1993.
20. Burrell, C.F., Schlachter, A.S., Pyle, R.V., and Searle, C.E., "Summary Abstract: Measurement of Impurities in a Neutral Beam by Laser Induced Fluorescence," *J. Vacuum Science and Technology A*, Vol. 2, No. 2, 1984, pp. 708-709.
21. Crofton, M.W., and Moore, T.A., unpublished results.
22. Marinero, E.E., Vasudev, R., and Zare, R.N., "The E, F $^1\Sigma_g^+$ Double-Minimum State of Hydrogen: Two-Photon Excitation of Inner and Outer Wells," *J. Chemical Physics*, Vol. 78, No. 2, 1983, pp. 692-699.
23. Rudolph, J., and Helbig, V., "Lifetimes of Excited States of Neutral titanium and Vanadium," *J. Physics B: Atomic and Molecular Physics*, Vol. 15, 1982, pp. L599-L602.
24. Ramaswami, S., Reeves, R.R., Rutten, M., and Halstead, J.A., "A Spectroscopic Study of Vapor-Phase Titanium," *J. Quantitative Spectroscopy and Radiative Transfer*, Vol. 49, No. 3, 1993, pp. 303-310.
25. Williamson, T.P., Martin, G.W., El-Astal, A.H., Al-Khateeb, A., Weaver, I., Riley, D., Lamb, M.J., Morrow, T., and Lewis, C.L.S., "An Investigation of Neutral and Ion Number Densities within Laser-Produced Titanium Plasmas in Vacuum and Ambient Environments," *Applied Physics A*, Vol. 69, 1999, pp. S859-S863.
26. Williams, G.J. Jr., Smith, T.B., Domonkos, M.T., Gallimore, A.D., and Drake, R.P., "Laser Induced Fluorescence Characterization of Ions Emitted from Hollow Cathodes," *IEEE Transactions on Plasma Science*, Vol. 28, No. 5, 2000, pp. 1664-1675.
27. Lins, G. and Hartmann, W., "Metal Vapour Densities in Pseudospark Switches with Tantalum Carbide Cathodes," *J. Physics D: Applied Physics*, Vol. 26, 1993, pp. 2154-2158.
28. Crofton, M.W., "Preliminary Mass Spectrometry of a Xenon Hollow Cathode," *J. Propulsion and Power*, Vol. 16, No. 1, 2000, pp. 157-159.
29. Dickie, L.O., and Kelly, F.M., "Lifetimes and Oscillator Strengths in Atomic Barium," *Canadian J. of Physics*, Vol. 49, 1971, pp. 2630-2632.
30. Bhattacharya, A.K., "Measurement of Barium Loss from a Fluorescent Lamp Electrode by Laser-Induced Fluorescence," *J. Applied Physics*, Vol. 65, No. 12, 1989, pp. 4595-4602.
31. Odintzova, G.A., and Striganov, A.R., "The Spectrum and Energy Levels of the Neutral Atom of Boron (B I)," *J. Physical and Chemical Reference Data*, Vol. 8, No. 1, 1979, pp. 63-67.
32. O'Brian, T.R., and Lawler, J.E., "Radiative Lifetimes in BI using Ultraviolet and Vacuum-Ultraviolet Laser-Induced Fluorescence," *Astronomy and Astrophysics*, Vol. 255, 1992, pp. 420-426.
33. Bredohl, H., Dubois, I., Houbrechts, Y., and Nzohabonayo, P., "New Analysis of the $A^3\Pi_i$-$X^3\Pi_i$ Transition of BN," *J. Molecular Spectroscopy*, Vol. 112, 1985, pp. 430-435.
34. Nakayama, Y., Kimura, T., Koyama, K., and Sasao, H., "Observation of Tungsten Particles in Vacuum Arcs by Laser Induced Fluorescence," *IEEE Transactions on Plasma Science*, Vol. 27, No. 4, 1999, pp. 906-910.
35. Lins, G., "Measurement of the Tungsten Ion Concentration after Forced Extinction of a Vacuum Arc," *IEEE Transactions on Plasma Science*, Vol. 17, No. 5, 1989, pp. 672-675.
36. Clawson, J.E., and Miller, M.H., "Experimental Transition Probabilities for Neutral and Singly Ionized Tungsten," *J. Optical Society of America*, Vol. 63, No. 12, 1973, pp. 1598-1603.
37. Duquette, D.W., Salih, S., and Lawler, J.E., "Radiative Lifetimes in WI using a Novel Atomic-Beam Source," *Physical Review A*, Vol. 24, No. 5, 1981, pp. 2847-2850.
38. Cook, T.B., King, P.W., and Roberto, J.B., "Summary Abstract: Measurement of the Ionization Length for Neutral Iron near the Wall in the ISX-B Tokamak using Laser-Induced Fluorescence," *J. Vacuum Science and Technology A*, Vol. 2, No. 2, 1984, pp. 707-708.
39. Bermudez, V.M., Hudgens, J.W., and Hoffbauer, M.A., "Detection of Iron in Lithium Niobate by Laser-Induced Fluorescence of Sputtered Atoms," *Applied Optics*, Vol. 22, No. 23, 1983, pp. 3681-3683.
40. Schweer, B., and Bay, H.L., "On the Velocity Distribution of Excited Fe-Atoms by Sputtering of Iron," *Applied Physics A*, Vol. 29, 1982, pp. 53-55.
41. Das, P., Ondrey, G., van Veen, n., and Bersohn, R., "Two Photon Laser Induced Fluorescence of Carbon Atoms," *J. Chemical Physics*, Vol. 79, No. 2, 1983, pp. 724-726.